AJNR

Diffusion Tensor Imaging in Lissencephaly

Nancy Rollins, Tony Reyes and Jon Chia

AJNR Am J Neuroradiol 2005, 26 (6) 1583-1586
http://www.ajnr.org/content/26/6/1583

AJNR Am J Neuroradiol 26:1583–1586, June/July 2005

Case Report

Diffusion Tensor Imaging in Lissencephaly

Nancy Rollins, Tony Reyes, and Jon Chia

Summary: Lissencephaly is a rare brain malformation characterized histologically by arrested neuronal migration such that the brain resembles that of a fetus before 23–24 weeks gestation. We studied a neonate with lissencephaly by using diffusion tensor imaging and suggest the dysplastic densely cellular layer IV is visible as a band of anisotropic diffusion. Fiber tracking showed lack of connectivity between the cortex and deep white matter and an abnormal limbic system.

Diffusion tensor imaging (DTI) is a relatively new MR technique in which image contrast is provided by diffusion anisotropy, the inherent preferential directional movement of water within the brain (1–6). DTI provides information about white matter organization and architecture not possible with conventional MR (5, 6). Diffusion tensor data are displayed as two-dimensional (2D) color maps in which image brightness indicates diffusion anisotropy whereas color indicates tract orientation (1–6). Fiber tracking may be done by the interrogation of regions on the color maps for fibers having a minimal fractional anisotropy (FA) set by the user (4–6); the resultant 3D image shows axonal projections. DTI and fiber tracking has been used to study white matter tracts in patients with holoprosencephaly and callosal agenesis (7, 8) and may provide insight into other congenital brain malformations in which cortical abnormalities are associated with abnormal white matter. We report DTI and fiber tracking in an infant with isolated lissencephaly.

Case Report

The lissencephalic patient was a 30-day-old Latin American male who presented with drooling and eye rolling that progressed from partial to secondary generalized seizure activity. The infant was the product of a nonconsanguineous marriage between healthy parents and had been delivered by elective repeat Caesarean section after an uncomplicated full-term pregnancy. There was no family history of birth defects or neurologic problems. There were two normal siblings, one male and one female. The patient had no cranial or facial dysmorphism. Fluorescence in situ hybridization done by using a probe specific for Miller-Dieker syndrome showed the short arm of chromosome 17 (17p13.3) was normal. There was a normal 46 XY karyotype. No further genetic analysis was conducted.

DTI was performed in accordance with institutional investigational review board requirements, and informed consent was obtained. MR imaging was acquired under conscious sedation by using a 1.5-T MR unit (Intera Release 9, Philips Medical Systems, Best, the Netherlands) with 30 mT/m gradients and slew rate of 150 T/m/ms, by using the standard quadrature head coil operating in receive mode. Conventional MR images included sagittal and axial T1 spin-echo sequences (400/25/2, TR/TE/signal intensity averages) and axial T2 fast spin-echo (4500/90/3). DTI was acquired with a six-channel SENSE head coil operating in receive mode applying high-angular-resolution diffusion imaging (2) isotropic diffusion-weighted gradients by using single-shot spin-echo planar sequence with a SENSE factor of 2.5 and an echo-planar imaging factor of 35. Other parameters were $b = 700$, 7357/98 (TR/TE), scan matrix 112×256, 246×246 mm FOV, 55 sections, 2.2-mm section thickness, no gap, 32 diffusion weighting directions. The DTI sequence was repeated three times by using one signal intensity average for a total image acquisition time of 13 minutes. A T1-weighted fast field echo with an inversion prepulse (15/4.7/20, TR/TE/flip angle) was acquired by using the same image resolution as the DT images to facilitate anatomic correlation.

The raw data from the DTI sequences and the anatomic coregistration images were transferred to an off-line PC having Philips Research Imaging Development Environment (PRIDE) software version 4.1V3 for image registration and fiber tracking. The three DTI raw data sets were processed by using the Diffusion Registration Tool Release 0.4. Automated section-by-section registration was performed for each individual acquisition, correcting for motion between sections and between acquisitions. The three corrected data sets were averaged together and saved as a new raw data file. Fiber tracking was generated by using the FA continuous tracking (or FACT) algorithm (4). Tracking was initiated by manually placing a region of interest within anatomically similar regions of cerebral cortex in the lissencephalic and normal brains. Tracking was performed from all pixels inside the regions of interest by using a "brute force" approach. Separate regions of interest were drawn to enclose the cingulum and fornix as has been described elsewhere (6). Tract propagation was terminated at a FA value of 0.15 and when the internal angle was 0.75.

Results

The routine MR images in the lissencephalic brain showed failure of operculation with absence of gyration. The cortex was markedly thickened and uniformly hypointense on the T2 images with the exception of a thin band of superficial increased T2 signal intensity (Fig 1A). The corpus callosum was intact, although subjectively thin, and the contents of the posterior fossa were normal. The axial 2D color maps showed thick symmetric bands of red in the frontoparietal regions, which represent structures preferentially oriented in a right-left direction (Fig 1B), whereas in the frontal poles the bands were green, which indicate anteroposterior orientation. Over the

Received May 25, 2004; accepted after revision August 20.

From the Department of Radiology, Children's Medical Center (N.R., T.R.), and the University of Texas Southwestern Medical Center (N.R.), Dallas, TX; and Philips Medical Systems (J.C.), Best, the Netherlands.

Address correspondence to Nancy Rollins, MD, Department of Radiology, Children's Medical Center, 1935 Motor Street, Dallas, TX 75235.

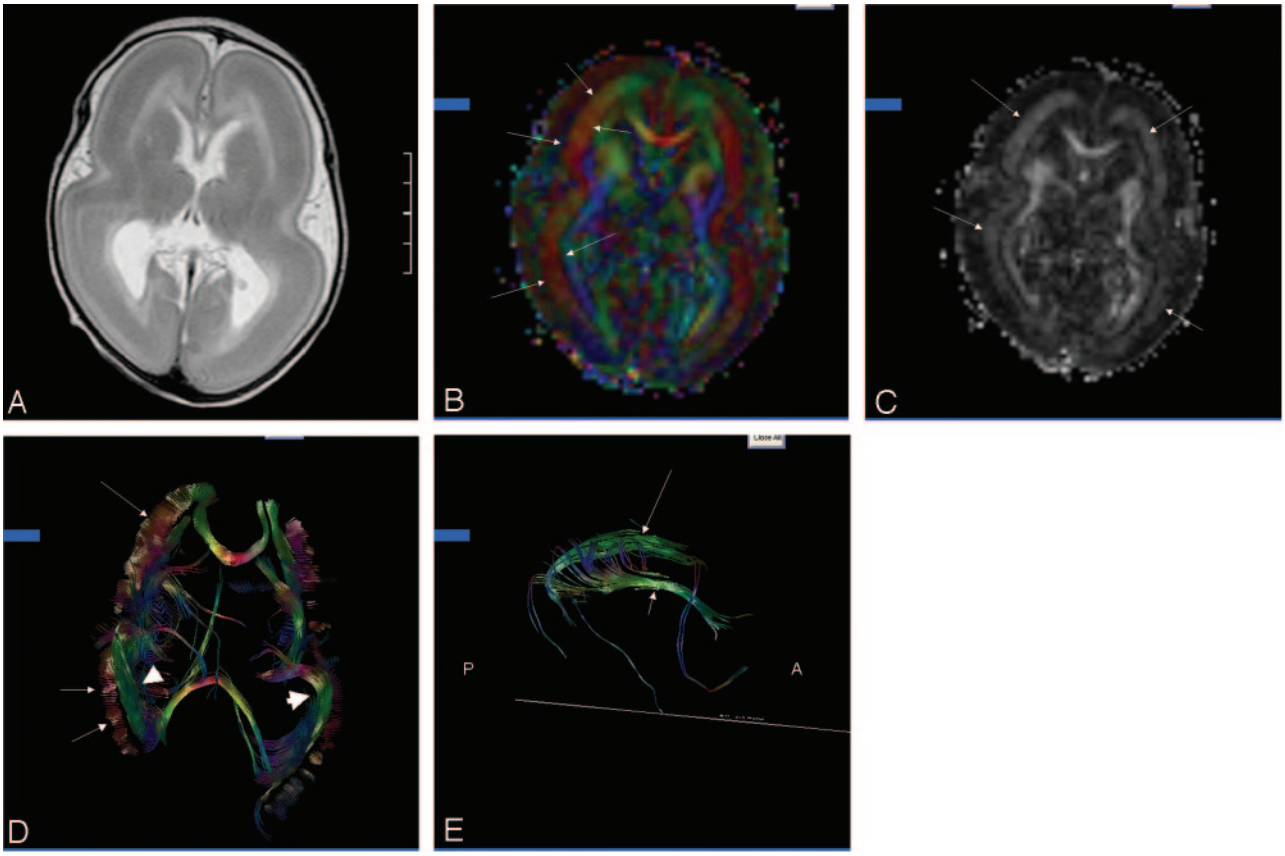

FIG 1. Patient, a 30-day-old male with isolated lissencephaly.
A, Axial T2-weighted image shows diffuse thickening of the cortex with lack of sulcation.
B, Axial 2D color map through the body of the lateral ventricles shows bands of color (*arrows*) corresponding to the deep cortex.
C, Axial anisotropy map shows bands of higher anisotropy corresponding to the bands of color (*arrows*) seen on the color maps.
D, Axial 3D presentation of corpus callosum, fronto-occipital fasciculus (*short* arrows), and presumed cell layer IV (*arrows*).
E, Sagittal 3D depiction of the cingulum (*long arrow*) and fornix (*short arrow*). Note absence of the temporal projections of the cingulum and fornix.

cerebral convexities, the presence of blue indicated a preferential cephalo-caudad orientation. The bands of color corresponded to areas of increased anisotropy on the FA maps (Fig 1C). Tractography showed the bands of color as thick, brushlike fibers (Fig 1D). There was minimal connectivity between the cortex and the deep white matter or between adjacent brushlike fibers on sequential sections. The columns of the fornix and the rostral and superior portions of the cingulum were visible, whereas the temporal portions of the limbic system were not (Fig 1E).

Discussion

DTI characterizes the 3D movement of water (1–6). Directionality is specified by the eigenvectors, whereas the eigenvalues specifies the rate of diffusion (1). The 2D color maps show the eigenvectors associated with the highest eigenvalues; color is used as an indicator of fiber orientation (2, 3). On the anisotropy maps, regions of brain having high degrees of spatial anisotropy show increased signal intensity. In the normal neonate, the deep and periventricular white matter show low anisotropy (9, 10). DTI studies of neonates and children during the 1st decade of life have shown that fractional anisotropy increases with age, especially in white matter (9, 10). The increasing spatial anisotropy is thought to be due to decrease in brain water content, the formation of new barriers to water mobility, such as cell membranes associated with the outgrowth of axons and dendrites and glial processes, and white matter myelination (9, 10). Gray matter has low anisotropy because of the lack of any preferred spatial orientation of the arborization of neurons and glia (9).

The normal cerebral cortex is composed of six horizontal cell layers (11, 12). Around 8 weeks gestation, neuroblasts begin to proliferate and associate with specialized bipolar glial cells having one process that extends toward the ventricular surface and another toward the pial surface (12). Receptors and ligans allow signaling between the migrating neuroblasts and the radial glial fibers; the bipolar glial cells provide scaffolding on which radial neuronal migration from the germinal layer to the cortical mantle occurs (11–13). In an "inside-out" sequence of neuronal migration, newly formed cells migrate outward through pre-existing cell layers to reach superficial cortex. The deepest layer of neocortex is normally populated first, whereas subsequent neuronal migration populates

more superficial layers of the neocortex. By 6–8-months gestation, the formation of the normal neocortex is complete (11). Detectable anisotropy has been shown in the normal developing human cerebral cortex from 24 to 32 weeks gestational age, when the parallel organization of radial glial fibers exists (14). Later in gestation, the high spatial organization of the neocortex is lost as the axons, dendrites, and glial processes course circuitously through the cerebral cortex, providing intracortical connectivity and connectivity between cortex and white matter (11).

Lissencephaly is a devastating brain malformation associated with seizures, profound developmental delay, and death in early childhood (15, 16). Lissencephalic patients with dysmorphic facial features usually have the Miller-Dieker syndrome (MDS), and patients with normal facial features usually have isolated classical lissencephaly. MDS is associated with deletions of chromosome 17p13.3 involving the LIS1 gene (13, 15, 16). The LIS1 mutation is thought to be associated with loss of dynein function, which is responsible for cytoplasmic function and nuclear movement during neuronal cell migration and axonal guidance; the cells with longest migration path are most affected. LIS1 may also affect cell proliferation (13, 16). About 40% of patients with isolated lissencephaly have submicroscopic deletions or intragenic mutations occurring at the 17p13.3 chromosome (13). The doublecortin gene, which maps to chromosome Xq22.3-q23, has also been found in patients with classic lissencephaly as well as in patients with subcortical band heterotopia (13). The patient described herein with isolated lissencephaly had no abnormalities of the 17p13.3 chromosome, although further genetic testing was not performed.

Grossly, the lissencephalic brain has total or near complete absence of sulcation (11, 15). Pathologic evaluation of the lissencephalic cortex has shown four-, instead of the normal six-, layer cortex (15). The two most superficial layers of cortex are formed by the neurons that migrated normally early in gestation, while the deeper layers are composed of neurons in migratory arrest (11, 15). The 3rd layer contains astrocytes, oligodendroglial cells, and dysplastic neurons, and the thickest, densely cellular 4th layer shows radial orientation, limited cellular differentiation, and no lamination (11, 15). Comparison between the anatomic images and the information acquired with DTI in the lissencephalic brain presented herein suggest the brushlike fibers represent the densely cellular 4th layer. The persistent parallel organization of glial fibers in the lissencephalic brain appears visible by DTI and tractography. The extensive intracortical connectivity and the connectivity between the cortex and the deep white matter fails to develop in lissencephaly, as evidenced by lack of visible subcortical white matter seen by tractography compared with that seen in the normal infant.

The surface of the hippocampus is covered by the alveus, which is composed of axons from the cells of the hippocampus and whose fibers converge to form the fibria of the fornix (6, 17). Normal hippocampal formation commences at about 10 weeks gestation, and the final configuration of the normal hippocampus depends on normal growth of the neocortex (17). In one report in which developmental changes in the hippocampus were studied by MR in patients with other congenital brain malformations, most patients with abnormal hippocampal formations had associated developmental abnormalities of the cerebral cortex (18). In the lissencephalic brain reported herein, that portion of the cingulum cephalad to the corpus callosum was seen with fiber tracking, but the temporal portion was not. Similarly, the columns of the fornix were visible, but the fibria appeared deficient. The temporal portions of the cingulum and fornix may in fact be present in the lissencephalic brain but not be visible, because of the limited image resolution currently provided by DTI. Apparent absence of the temporal portions of the limbic system as seen by DTI has also been reported in patients with holoprosencephaly, whereas morphologic abnormalities of the hippocampus have been documented in patients with lissencephaly by routine MR imaging (7, 18). Whether the abnormal hippocampus that forms in the lissencephalic brain induces dysplastic or incompletely formed limbic system is not known.

In conclusion, DTI appears to be sensitive to the presence of regions of dysplastic cortex having relatively high fractional anisotropy and to the detection of a malformed limbic system. Further refinement of the DTI parameters is needed to improve spatial resolution and further application of this technique into patients with various forms of cortical dysplasia is indicated.

References

1. Dong Q, Welsh RC, Chenevert TL, et al. **Clinical applications of diffusion tensor imaging.** *J Magn Reson Imaging* 2004;19:6–18
2. Ozarslan E, Mareci TH. **Generalized diffusion tensor imaging and analytical relations between diffusion tensor imaging and high angular resolution imaging.** *Mag Reson Med* 2003;50:955–965
3. DaSilva AFM, Tuch DS, Weigell MR, Hadjikhani N. **A primer on diffusion tenor imaging of anatomical substructures.** *Neurosurg Focus* 2003;15:1–4
4. Mori S, Crain BJ, Chacko VP, van Zijl. **Three-dimensional tracking of axonal projections in the brain by magnetic resonance imaging.** *Ann Neurol* 1999;45 265–269
5. Jellison BJ, Field AS, Medow J, et al. **Diffusion tensor imaging of cerebral white matter: a pictorial review of physics, fiber tract anatomy, and tumor imaging patterns.** *AJNR Am J Neuroradiol* 2004;25:356–369
6. Wakana S, Jiang H, Nagae-Poetscher LM, van Zijll PCM, Mori S. **Fiber tract-based atlas of human white matter anatomy.** *Radiology* 2004;230:77–87
7. Albayram S, Melhem ER, Mori S, et al. **Holoprosencephaly in children: diffusion tensor MR imaging of white matter tracts of the brainstem: initial experience.** *Radiology* 2002;223:645–651
8. Seung-Koo Le, Mori S, Kim Dong J, et al. **Diffusion tensor MR imaging visualizes the altered hemispheric fiber connection in callosal dysgenesis.** *AJNR Am J Neuroradiol* 2004;25:25–28
9. Mukherjee P, Miller JH, Shimony JS, et al. **Normal brain maturation during childhood: developmental trends characterized with MR.** *Radiology* 2001;221:349–358
10. Schmithorst VJ, Wilke M, Dardzinski BJ, Holland SK. **Correlation of white matter diffusivity and anisotropy during childhood and adolescence: a cross-sectional diffusion tensor imaging study.** *Radiology* 2002;222:212–218
11. Pilz D, Stoodley N, Golden JA. **Neuronal migration, cerebral cortical development, and cerebral cortical anomalies.** *J Neuropathol Exp Neurol* 2002;61:1–11

12. Rakie P. **Mode of cell migration to the superficial layers of the fetal monkey cortex.** *J Comp Neurol* 1972;145:61–83
13. Pilz DT, Matsumoto, Minnerath S, et al. **LIS1 and XLIS (DCX) mutations cause most classical lissencephaly but different patterns of malformation.** *Hum Mol Genet* 1998;8:1757–60
14. Neil JJ, McKinstry RC, Schlaggar BL, et al. **Evaluation of diffusion anisotropy during human cortical grey matter development.** *Proceedings of the Eighth Meeting of the International Society for Magnetic Resonance in Medicine.* Denver, Colorado. April 1–7, 2000;1:591.
15. Landrieu P, Husson B, Pariente D, Lacroix C. **MRI-neuropathological correlations in type I lissencephaly.** *Neuroradiol* 1998;40: 173–176
16. Fogli A, Guerrini R, Moro F, et al. **Intracellular levels of the LIS1 protein correlate with clinical and neurological findings in patients with classical lissencephaly.** *Ann Neurol* 1999;45:154–161
17. Carpenter MB. *Core text of neuroanatomy.* 3rd ed. Baltimore: Williams & Wilkins;1985:332–339
18. Sato N, Hatakeyama S, Shimizu A, et al. **MR evaluation of the hippocampus in patients with congenital malformations of the brain.** *AJNR Am J Neuroradiol* 2001;22:389–393